PORTIONS OF THIS DOCUMENT ARE ILLEGIBLE

LA-UR -78-196

CONF-780117--1

TITLE: SOLAR OPACITY AND EQUATION OF STATE

AUTHOR(S): W. F. Huebner

SUBMITTED TO: For the proceedings of the Solar Neutrino Conference held at Brookhaven, January 5 through January 7, 1978.

MN ONLY

los alamos
scientific laboratory
of the University of California
LOS ALAMOS, NEW MEXICO 87545

An Affirmative Action/Equal Opportunity Employer

Form No. 836
St. No. 2629
1/78

UNITED STATES
ENERGY RESEARCH AND
DEVELOPMENT ADMINISTRATION
CONTRACT W-7405-ENG. 36

EAB

SOLAR OPACITY AND EQUATION OF STATE

W. F. Huebner
Theoretical Division, T-4
University of California, Los Alamos Scientific Laboratory

Abstract

The disadvantages of radiative diffusion over radiative transfer in the photosphere as used in structure calculations is reemphasized. Uncertainties in the opacity due to uncertainties in chemical composition and in approximations of the physics are described and estimated. Internal consistency of equation of state and opacity is recommended.

Energy produced by nuclear reactions in the inner core of the sun is transported primarily in form of photon radiation outward to the photosphere and corona. There the energy manifests itself through luminosity and to a smaller measure through the solar wind. Opacity determines the rate of diffusion of the energy which in turn determines the temperature gradients and to a lesser degree the temperature in the core. Since some nuclear reactions that produce neutrinos depend sensitively on conditions in the solar interior, opacity and equation of state (EOS) directly affect solar neutrino production.[1]

I will not describe the details of opacity calculations; for astrophysics this has been done in several earlier papers.[2-5] Instead, I will discuss sources of uncertainties connected with opacities and indicate limits of accuracy, where possible, in regard to the following aspects:

(1) Radiative diffusion vs. radiative transfer in the photosphere.

(2) Changes of opacity due to changes in total metals mass abundance Z relative to hydrogen and helium.

(3) Changes of opacity due to changes in relative abundances of metals relative to each other (constant Z).

(4) Changes of opacity due to multipole radiation, relativity, collective effects, and electron conduction.

(5) Internal consistency of equation of state (EOS) and opacity.

Before going into the details the standard for comparison must be defined. The opacities presented here for temperatures above 1 eV were obtained from our Astrophysical Opacity Library.[6] This Library is based on two models for the ions: the explicit ion model for temperatures less than about 100 eV* and on the mean ion model for higher temperatures and

*1 eV = 11605 K

for some of the higher densities at the lower temperatures. Experimental data and screening constants are used in the atomic structure determinations. Opacities based on these models for individual elements heavier then Mg are in good agreement with opacities based on models using a Thomas-Fermi potential. The usual processes for opacity calculations are considered: photoionization, inverse bremsstrahlung, line absorption and scattering.

(1) Radiative diffusion vs. radiative transfer in the photosphere.

Recently Ulrich and Rhodes[7] pointed out that even though the structure of the solar envelope does not influence the interior structure directly, it does determine the mixing-length parameter for the convective zone. Since the mixing-length parameter is sensitive to the composition of the solar mixture, it is then possible to test the low-Z (low metal abundance) solar model that had been invented to explain the lack of detection of solar neutrinos. The effect of low-Z on opacity is described in the next section. Here I want to make a few remarks about radiative transfer vs. diffusion that may affect the solar envelope.

The diffusion approximation to radiation flow is appropriate for conditions where local thermodynamic equilibrium (LTE) is valid and the gradient of the net radiation flux normal through a surface, $dF_\nu(\vec{r})/dr_n$, is small. Under those conditions

$$1/4 \frac{dF_\nu(\vec{r})}{dr_n} = \rho \kappa_\nu^{(a)} \left[B_\nu(T,\vec{r}) - J_\nu(\vec{r})\right] , \qquad (1)$$

is about zero and the zeroth moment (or angle averaged) intensity is $J_\nu(\vec{r}) \approx B_\nu(T,\vec{r})$. This leads to the Rosseland mean opacity

$$\kappa_R^{-1} = \int_0^\infty [\kappa_\nu^{-1} \partial B_\nu(T)/\partial T]d\nu / \int_0^\infty [\partial B_\nu(T)/\partial T]d\nu \ . \qquad (2)$$

In these equations κ_ν is the mass extinction (absorption corrected for stimulated emission plus scattering) coefficient, $\kappa_\nu^{(a)'}$ the mass absorption coefficient corrected for stimulated emission (both depend on density ρ and temperature T) and B_ν is the Planck intensity function. These conditions apply in the solar interior but not in the photosphere. More precisely, the Rosseland opacity applies only under LTE conditions at depths Δr_{max} below the photosphere where the optical depth

$$\tau_\nu = \int_{\Delta r} \kappa_\nu \, dr \ , \qquad (3)$$

at frequencies ν <u>between</u> spectral absorption lines is <u>large</u> compared to 1.

If, on the other hand, the magnitude of the flux gradient is large (e.g., $J_\nu \approx 0$), then the Planck mean opacity

$$\kappa_P = \int_0^\infty \kappa_\nu B_\nu(T) \, d\nu / \int_0^\infty B_\nu(T)d\nu \ , \qquad (4)$$

is obtained. But the flux gradient is large at all frequencies only if the optical depth, Eq. (3), is <u>small</u> at physical depth Δr_{min} at the <u>centers</u> of the strongest absorption lines. Δr_{min} and Δr_{max} are measured inward from the photosphere (or from some point $\vec{r}$ at which $B_\nu(T,\vec{r}) \approx 0$). There is no easily defined grey opacity that applies between Δr_{min} and Δr_{max}.

Many structure calculations match the observed solar luminosity, but ignore the details of the boundary layers particularly in the lower photosphere. Some atmosphere models correct this with line blanketing or opacity distribution function approximations or a statistical sampling procedure. None of these go smoothly over into the Rosseland mean opacity with in-

creasing depth. Planck and Rosseland group mean opacities coupled with an interpolation scheme that gives Planck opacities at Δr_{min} and Rosseland opacities at Δ_{max} has apparently not been tried. The larger the number of photon energy groups is the closer the two mean opacities approach one another and the closer the calculation approaches radiative transfer.

Table I, column A is the solar metal abundance as taken from Cameron's compilation[8] that was used in calculations of the low temperature opacities and EOS presented in Table II for X = 0.770, Y = 0.212, Z = 0.018. Some of the more important molecular transitions have been included in this table. Figure 1 illustrates the extinction coefficient as a function of photon energy at a typical temperature and density. Group mean opacities, not presented here, can be formed from such calculations. The non-LTE conditions in the chromosphere and in the corona must still be considered separately. Perhaps the convection zone below the photosphere introduces greater uncertainties in the flux and temperature profile than these improvements warrant.[7]

(2) Changes of opacity due to changes in total metals mass abundance Z relative to hydrogen and helium.

A reference set of opacities, presented in Table III, was calculated for a mixture with X = 0.770, Y = 0.212, Z = 0.018 and a set for a metal poor mixture is presented in Table IV for X = 0.8832, Y = 0.1150, Z = 0.0018. The relative composition of the metals for these two calculations is presented in Table I, Column A. The maximum difference of opacity of the metal poor to the reference mixture is 80% at kT ≈ 200 eV, in the density range 0.2 to 1.0 g/cm^3. A contour map of the logarithm of the Rosseland opacity for the reference set is shown in Fig. 2 as a function of density and temperature. The bumps are due to the shell structure of the

constituent elements. Also shown are the conditions for the standard solar model as a function of radius.[9] Consulting this map it is seen that the maximum change of opacity due to the above change in metal abundance occurs at 0.6 $R_\odot$ of the standard model. Curve A in Fig. 3 illustrates the relative difference of opacities at temperature-density points as function of solar radius.

(3) Changes of opacity due to changes in relative abundances of metals relative to each other (constant Z).

To check the sensitivity of opacity, to changes of abundances of metals with respect to each other a calculation was made using the abundances in Column B in Table I. These abundances correspond to those given by Allen.[9] It should be kept in mind that all these calculations are done with the Astrophysical Opacity Library.[6] This implies that the basic equation of state and opacity data for each constituent element is the same regardless of the relative proportions in the mixture. This could never be guaranteed in previous calculations which always started from scratch. The maximum change of opacity relative to the reference case is 13% at $kT \approx 300$ eV and $\rho \approx 0.1$ g/cm^3. Additional maxima of 12% occur at $kT \approx 60$ eV and $\rho \approx 1 \times 10^{-3}$ g/cm^3 and at $kT \approx 1.5$ keV and $\rho \approx 100$ g/cm^3. The relative difference of opacities at temperature - density points as a function of radius in the standard solar model is shown in Fig. 3, curve B.

As a further test the elements P, Cl, Ti and Mn were removed from the list given in Table I, Column A and the abundance of Fe was increased to include the abundances of Cr and Ni. The metal abundance was then renormalized to give Z = 0.018. The maximum reduction of opacity relative to the reference mixture was about 6%. This test serves as a sensitivity indicator for completeness of chemical composition.

(4) Changes of opacity due to multipole radiation, relativity, collective effects, and electron conduction.

When the photon wavelength is comparable or smaller than the size of the ions, then the dipole approximation of the matrix elements for cross sections is insufficient. Multipole contributions to the opacity become important for conditions found near the center of the sun. Contributions to the matrix elements due to relativistic effects involve the same parameters. Multipole and relativistic contributions should therefore be considered together. These effects had in the past not been included in solar opacities; they have been included in the bound-free contributions to the opacities as presented here. Figure 4 illustrates the mass extinction coefficients as a function of reduced photon energy $u \equiv h\nu/kT$ at densities and temperatures found in the standard solar model. Reading from the bottom up the curves correspond approximately to distances 0, 0.2, 0.4, 0.6, 0.8, 0.9, 0.95, 0.995 times the solar radius $R_\odot$ as measured from the sun's center. The Rosseland weighting function, appropriate for all these extinction coefficient curves, is plotted at the top of Fig. 4. At kT = 1.25 keV important bound-free cross sections influenced by multipole and relativity effects contribute to the extinction above $u \approx 6$ where the Rosseland weighting function is rapidly decreasing. At lower temperatures these contributions add-in at still higher u values and thus become even less important.

Collective effects to scattering have been described by Watson.[10] These effects reduce the scattering cross section in high density plasmas at high photon energies. Since scattering is not a dominant process where the Rosseland weighting function is large even at the highest temperatures in the sun, the reduction of the opacity is only a few percent.

Table V presents opacities due to electron conduction. The largest effect on the total Rosseland opacity

$$\kappa_T = (\kappa_R^{-1} + \kappa_C^{-1})^{-1} , \qquad (5)$$

at temperatures and densities appropriate to the standard solar model is a reduction by about 0.5%. κ_R and κ_C are the radiative and conductive opacity, respectively.

The net effect from all corrections is small since they tend to cancel.

(5) Internal consistency of equation of state (EOS) and opacity.

Sensitivity of the solar neutrino flux to changes in opacity and EOS has been investigated by Bahcall et al.[11] They found that the neutrino flux is much more sensitive to local EOS changes than it is to local opacity changes. In their analysis EOS and opacity were treated as independent quantities, while in fact (for a constant composition) they are not. Comparing the two mixtures presented in Table I the relative differences of opacity as a function of solar radius are shown by curve B in Fig. 3. In contrast the relative differences in the EOS are less than ±0.1%. Although uncertainties of EOS have a much bigger effect on solar neutrino production then opacities have, the uncertainties of opacities are much larger. It appears that solar structure calculations have not been carried out with an internally consistent set of EOS and opacity. The tables provided here are internally consistent and show the effects of shell structure at low temperatures. At conditions appropriate to the deep solar interior, shell structure effects due to the heavier constituents are not clearly discernible, but bumps of the order of a few percent cannot be ruled out.

Summary.

There does not exist a single experimental verification of opacities in the temperature-density region of interest to solar structure. This is so because opacity is nonlinear with respect to plasma properties such as the density and temperature and attempts to measure these to the required accuracy have failed. LTE and optical depth requirements restrict the experimental range and fluiddynamic coupling greatly complicates interpretation of experiments.

All opacities are obtained from calculations based on well founded theory. Some experimental data for cross sections and energy levels are used; but even these data are incomplete and often very sparse and must be supplemented with calculated values which are fitted or normalized to experimental data in neighboring regions. As is the case in most calculations, approximations must be made to keep problems tractable. Thus, experimental errors in the data and uncertainties due to approximations must be combined in the error analysis. For this purpose I have tabulated the uncertainties for relative abundance between metals (Fig. 3, curve B), uncertainties for relative abundance in terms of X-Y-Z, the errors in basic opacity data and uncertainties in the atomic model approximations. It is extremely difficult to make a complete, quantitative analysis. Although only very few opacity programs can handle general astrophysical mixtures, about ten programs have been available to make comparisons for individual elements or simple mixtures in overlapping regions of density, temperature and atomic number. Four of these opacity programs exist at Los Alamos. Various independent investigators have made comparisons using two of my programs: LEO (light elements opacity) and HEO (heavy element opacity) as a standard. In all comparisons most disagreements have been traced and

explained. LEO, based on a scaled Hartree-Fock model of the atom, and HEO, based on the Thomas-Fermi potential have also been compared with each other and are in good agreement (better than 30%) as already indicated in the introduction. From the general nature of these comparisons, and the many calculations, studies of results and improvements that we have made (see, e.g. Ref. 5) some rules have emerged to estimate opacity uncertainties. Uncertainty values are presented in Table VI as a function of solar radius appropriate to conditions in the standard model. Since the values in columns A and B depend on composition, they are correlated with radius. The values in columns C are based primarily on uncertainties of the partial photoelectric cross sections and the values in columns D take into account the complexity of the spectral structure as apparent in Fig. 4. Columns C and D depend on atomic structures (e.g. electronic occupation numbers) which change with temperature and are therefore uncorrelated.

I wish to acknowledge the collaboration of M. F. Argo, N. H. Magee, Jr., and A. L. Merts particularly in the production of tables and graphs.

References

1. J. N. Bahcall, W. F. Huebner, N. H. Magee, Jr. and A. L. Merts, Astrophys. J. 184, 1 (1973).
2. A. N. Cox, "Stellar Absorption Coefficients and Opacities," in Stellar Structure, Aller and McLaughlin, Eds., The University of Chicago (1965).
3. T. R. Carson, D. F. Mayer and D. ". N. Stibbs, Mon. Not. R. Astr. Soc. 140, 483 (1968).
4. T. R. Carson and H. M. Hollingsworth, Mon. Not. R. Astr. Soc. 141, 77 (1968).
5. N. H. Magee, Jr., A. L. Merts and W. F. Huebner, Astrophys. J. 196, 617 (1975).
6. W. F. Huebner, A. L. Merts, N. H. Magee, Jr. and M. F. Argo, "Astrophysical Opacity Library," Los Alamos Scientific Laboratory Manual LA-6760-M (1977).
7. R. K. Ulrich and E. J. Rhodes, Jr., Astrophys. J. 218, 521 (1977).
8. A. G. W. Cameron, Space Sci. Rev. 15, 121 (1973).
9. C. W. Allen, Astrophysical Quantities, 3rd edition, The Athlone Press, University of London (1973).
10. W. D. Watson, Astrophys. J. 158, 303 (1969).
11. J. N. Bahcall, N. A. Bahcall and R. K. Ulrich, Astrophys. J. 156, 559 (1969).

TABLE I

METAL NUMBER ABUNDANCES

	A	B
C	.2664	.2565
N	.0844	.0712
O	.4854	.5065
Ne	.0777	.0636
Na	.0014	.0014
Mg	.0240	.0206
Al	.0019	.0017
Si	.0226	.0257
P	.0002	.0003
S	.0113	.0124
Cl	.0001	.0003
Ar	.0026	.0049
Ca	.0016	.0015
Ti	.0001	.0001
Cr	.0003	.0006
Mn	.0002	.0002
Fe	.0187	.0310
Ni	.0011	.0015
	1.0000	1.0000

Low Temperature EOS and Opacities

ρ[g/cm^3]	kT[eV]	P[dyn/cm^2]	E[erg/g]	κ_R[cm^2/g]	κ_p[cm^2/g]
1 x 10^{-5}	5,000000E-01	3,88258E+06	2,68365E+12	8,38697E+00	1,92097E+01
	6,000000E-01	4,71794E+06	2,84899E+12	2,52162E+01	6,73396E+01
	8,000000E-01	6,33672E+06	3,14587E+12	2,24455E+02	9,66296E+03
	1,000000E+00	8,10656E+06	3,66792E+12	1,18435E+03	1,82598E+05
	1,250000E+00	1,10585E+07	5,18237E+12	4,82667E+03	4,30122E+05
	1,500000E+00	1,54144E+07	7,94110E+12	1,11449E+04	6,19429E+05
	2,000000E+00	2,64469E+07	1,39225E+13	1,83055E+04	4,21805E+05
3 x 10^{-6}	5,000000E-01	1,17791E+06	2,72398E+12	4,37625E+00	1,62614E+01
	6,000000E-01	1,41952E+06	2,86064E+12	1,52166E+01	4,87563E+01
	8,000000E-01	1,90838E+06	3,18687E+12	1,58453E+02	5,65697E+03
	1,000000E+00	2,48319E+06	3,92768E+12	8,85872E+02	1,85015E+05
	1,250000E+00	3,56795E+06	6,23896E+12	3,50966E+03	4,37742E+05
	1,500000E+00	5,18972E+06	9,98012E+12	6,77795E+03	4,81168E+05
	2,000000E+00	8,55021E+06	1,55720E+13	5,77376E+03	2,86334E+05
1 x 10^{-6}	5,000000E-01	3,93983E+05	2,73665E+12	2,11027E+00	1,15208E+01
	6,000000E-01	4,73679E+05	2,86649E+12	8,87651E+00	3,30494E+01
	8,000000E-01	6,39683E+05	3,25170E+12	1,89191E+02	3,52130E+03
	1,000000E+00	8,54256E+05	4,32917E+12	6,79966E+02	1,53718E+05
	1,250000E+00	1,30391E+06	7,66092E+12	2,46299E+03	4,44894E+05
	1,500000E+00	1,92465E+06	1,28126E+13	3,63950E+03	3,69657E+05
	2,000000E+00	2,96965E+06	1,65787E+13	2,30706E+03	1,85436E+05
3 x 10^{-7}	5,000000E-01	1,18344E+05	2,74161E+12	9,56460E-01	1,85881E+01
	6,000000E-01	1,42217E+05	2,87339E+12	5,81226E+00	2,73475E+01
	8,000000E-01	1,93928E+05	3,37620E+12	7,41450E+01	2,22159E+03
	1,000000E+00	2,70054E+05	5,06528E+12	5,80964E+02	9,09955E+04
	1,250000E+00	4,41505E+05	9,73402E+12	1,47954E+03	3,51939E+05
	1,500000E+00	6,31348E+05	1,38317E+13	1,43941E+03	2,43057E+05
	2,000000E+00	9,16208E+05	1,72,68E+13	6,49807E+02	5,29501E+04
1 x 10^{-7}	5,000000E-01	3,94647E+04	2,74374E+12	4,49428E-01	8,95479E+00
	6,000000E-01	4,74490E+04	2,88320E+12	3,05629E+00	2,63458E+01
	8,000000E-01	6,57121E+04	3,57406E+12	5,32260E+01	1,50200E+03
	1,000000E+00	9,73707E+04	6,13698E+12	3,65289E+02	4,39436E+04
	1,250000E+00	1,63765E+05	1,17774E+13	7,81954E+02	1,67930E+05
	1,500000E+00	2,20749E+05	1,48674E+13	5,28405E+02	9,68700E+04
	2,000000E+00	3,10472E+05	1,76968E+13	2,02894E+02	1,80445E+04
3 x 10^{-8}	5,000000E-01	1,18426E+04	2,74585E+12	2,84740E-01	7,42198E+00
	6,000000E-01	1,42582E+04	2,90186E+12	1,78082E+00	2,55645E+01
	8,000000E-01	2,03219E+04	3,94433E+12	3,76008E+01	8,28155E+02
	1,000000E+00	3,26383E+04	7,86393E+12	2,41159E+02	1,57276E+04
	1,250000E+00	5,34653E+04	1,35394E+13	3,88929E+02	3,62199E+04
	1,500000E+00	6,79592E+04	1,54707E+13	1,59643E+02	1,58900E+04
	2,000000E+00	9,40324E+04	1,79857E+13	5,78096E+01	2,55879E+03
1 x 10^{-8}	5,000000E-01	3,94860E+03	2,74869E+12	1,15224E-01	7,40416E+00
	6,000000E-01	4,76519E+03	2,93182E+12	1,07495E+00	2,78505E+01
	8,000000E-01	7,20614E+03	4,52716E+12	2,77591E+01	5,10554E+02
	1,000000E+00	1,22088E+04	9,85971E+12	1,45319E+02	7,55161E+03
	1,250000E+00	1,85022E+04	1,44381E+13	1,14396E+02	9,45022E+03
	1,500000E+00	2,29691E+04	1,58683E+13	5,40480E+01	5,02055E+03
	2,000000E+00	3,14715E+04	1,81065E+13	1,96650E+01	3,70519E+02

Table III A

Low Density Rosseland Opacity [cm^2/g], Energy [erg/g], Pressure [dyn/cm^2]

for X = 0.770, Y = 0.212, Z = 0.018

RHO	1.0000E-06	2.0000E-06	5.0000E-06	1.0000E-05	2.0000E-05	5.0000E-05	1.0000E-04	2.0000E-04	5.0000E-04
0(EV)	.6682E+03	.7878E+03	.9767E+03	.1153E+04	.1372E+04	0.	0.	0.	0.
	.4323E+13	.4047E+13	.3796E+13	.3665E+13	.3571E+13	0.	0.	0.	0.
	.8521E+06	.1668E+07	.4089E+07	.8097E+07	.1608E+08	0.	0.	0.	0.
5(EV)	.2464E+04	.3101E+04	.4014E+04	.4790E+04	.5664E+04	.7035E+04	.8300E+04	0.	0.
	.7634E+13	.6603E+13	.5711E+13	.5173E+13	.4764E+13	.4373E+13	.4172E+13	0.	0.
	.1296E+07	.2440E+07	.5715E+07	.1101E+08	.2138E+08	.5199E+08	.1025E+09	0.	0.
0(EV)	.3639E+04	.5519E+04	.8587E+04	.1123E+05	.1409E+05	.1820E+05	.2173E+05	.2600E+05	0.
	.1197E+14	.1070E+14	.9017E+13	.7900E+13	.6979E+13	.6034E+13	.5502E+13	.5123E+13	0.
	.1907E+07	.3571E+07	.8154E+07	.1530E+08	.2893E+08	.6805E+08	.1313E+09	.2559E+09	0.
0(EV)	.2324E+04	.4619E+04	.1065E+05	.1863E+05	.3014E+05	.5023E+05	.6873E+05	.9000E+05	0.
	.1643E+14	.1590E+14	.1487E+14	.1344E+14	.1265E+14	.1099E+14	.9819E+13	.8779E+13	0.
	.2938E+07	.5732E+07	.1371E+08	.2618E+08	.4[illegible]E+08	.1139E+09	.2140E+09	.4040E+09	0.
0(EV)	.1993E+04	.2967E+04	.7793E+04	.1559E+05	.2982E+05	.6409E+05	.1046E+06	.1500E+06	0.
	.1874E+14	.1851E+14	.1793E+14	.1730E+14	.1651E+14	.1518E+14	.1405E+14	.1286E+14	0.
	.3813E+07	.7527E+07	.1841E+08	.3593E+08	.6960E+08	.1649E+09	.3136E+09	.5917E+09	0.
0(EV)	.9456E+03	.2050E+04	.5638E+04	.1189E+05	.2450E+05	.5938E+05	.9976E+05	.1494E+06	.2600E+06
	.2019E+14	.2010E+14	.1985E+14	.1951E+14	.1903E+14	.1810E+14	.1717E+14	.1610E+14	.1452E+14
	.4628E+07	.9194E+07	.2267E+08	.4474E+08	.8804E+08	.2122E+09	.4091E+09	.7842E+09	.1829E+10
0(EV)	.5099E+03	.1056E+04	.2764E+04	.5682E+04	.1161E+05	.2869E+05	.5301E+05	.9012E+05	.1641E+06
	.2286E+14	.2270E+14	.2252E+14	.2235E+14	.2215E+14	.2174E+14	.2125E+14	.2060E+14	.1944E+14
	.6232E+07	.1239E+08	.3070E+08	.6087E+08	.1209E+09	.2979E+09	.5841E+09	.1142E+10	.2731E+10
0(EV)	.2407E+03	.5032E+03	.1294E+04	.2588E+04	.5099E+04	.1195E+05	.2141E+05	.3716E+05	.7129E+05
	.2686E+14	.2627E+14	.2560E+14	.2519E+14	.2484E+14	.2444E+14	.2410E+14	.2366E+14	.2294E+14
	.7943E+07	.1574E+08	.3806E+08	.7701E+08	.1526E+09	.3772E+09	.7468E+09	.1473E+10	.3577E+10
0(EV)	.1009E+03	.2174E+03	.5862E+03	.1211E+04	.2459E+04	.5926E+04	.1107E+05	.1937E+05	.3582E+05
	.3041E+14	.3012E+14	.2951E+14	.2889E+14	.2824E+14	.2745E+14	.2695E+14	.2647E+14	.2571E+14
	.9660E+07	.1922E+08	.4751E+08	.9401E+08	.1860E+09	.4585E+09	.9083E+09	.1797E+10	.4397E+10
0(EV)	.2901E+02	.6057E+02	.1690E+03	.3641E+03	.7738E+03	.2012E+04	.3944E+04	.7469E+04	.1554E+05
	.3566E+14	.3555E+14	.3537E+14	.3515E+14	.3484E+14	.3419E+14	.3353E+14	.3281E+14	.3172E+14
	.1295E+08	.2585E+08	.6432E+08	.1279E+09	.2544E+09	.6285E+09	.1243E+10	.2462E+10	.6046E+10
0(EV)	.1364E+02	.2767E+02	.7230E+02	.1539E+03	.3286E+03	.8639E+03	.1745E+04	.3309E+04	.7138E+04
	.4066E+14	.4055E+14	.4040E+14	.4025E+14	.4005E+14	.3967E+14	.3923E+14	.3871E+14	.3785E+14
	.1623E+08	.3230E+08	.8071E+08	.1604E+09	.3201E+09	.7946E+09	.1575E+10	.3128E+10	.7726E+10
0(EV)	.6642E+01	.1317E+02	.3439E+02	.7204E+02	.1502E+03	.3818E+03	.7374E+03	.1358E+04	.2801E+04
	.4688E+14	.4677E+14	.4663E+14	.4650E+14	.4632E+14	.4599E+14	.4562E+14	.4521E+14	.4442E+14
	.2032E+08	.4058E+08	.1012E+09	.2019E+09	.4023E+09	.9997E+09	.1985E+10	.3942E+10	.9791E+10
0(EV)	.3502E+01	.6440E+01	.1599E+02	.3331E+02	.6915E+02	.1749E+03	.3454E+03	.6835E+03	.1288E+04
	.5307E+14	.5298E+14	.5283E+14	.5264E+14	.5252E+14	.5218E+14	.5188E+14	.5150E+14	.5097E+14
	.2441E+08	.4876E+08	.1216E+09	.2428E+09	.4842E+09	.1203E+10	.2396E+10	.4773E+10	.1184E+11
0(EV)	.1387E+01	.2241E+01	.4770E+01	.8967E+01	.1777E+02	.4574E+02	.9112E+02	.1737E+03	.3672E+03
	.6541E+14	.6532E+14	.6517E+14	.6503E+14	.6487E+14	.6459E+14	.6431E+14	.6394E+14	.6334E+14
	.3259E+08	.6512E+08	.1625E+09	.3246E+09	.6480E+09	.1614E+10	.3217E+10	.6407E+10	.1591E+11
0(EV)	.8449E+00	.1196E+01	.2139E+01	.3649E+01	.6715E+01	.1653E+02	.3249E+02	.6329E+02	.1490E+03
	.7776E+14	.7764E+14	.7751E+14	.7736E+14	.7710E+14	.7690E+14	.7641E+14	.7629E+14	.7564E+14
	.4077E+08	.8147E+08	.2034E+09	.4064E+09	.8114E+09	.2023E+10	.4034E+10	.8035E+10	.1996E+11
0(EV)	.6243E+00	.8084E+00	.1280E+01	.1967E+01	.3331E+01	.7510E+01	.1480E+02	.2998E+02	.6994E+02
	.9015E+14	.9005E+14	.8989E+14	.8973E+14	.8953E+14	.8921E+14	.8891E+14	.8853E+14	.8792E+14
	.4895E+08	.9784E+08	.2444E+09	.4882E+09	.9750E+09	.2431E+10	.4851E+10	.9671E+10	.2406E+11
0(EV)	.4485E+00	.4975E+00	.6563E+00	.8846E+00	.1303E+01	.2561E+01	.4721E+01	.9326E+01	.2326E+02
	.1150E+15	.1148E+15	.1147E+15	.1145E+15	.1143E+15	.1140E+15	.1137E+15	.1132E+15	.1125E+15
	.6532E+08	.1306E+09	.3262E+09	.6519E+09	.1303E+10	.3251E+10	.6491E+10	.1294E+11	.3221E+11
0(EV)	.3948E+00	.4232E+00	.4869E+00	.5736E+00	.7349E+00	.1205E+01	.1990E+01	.3660E+01	.9219E+01
	.1399E+15	.1397E+15	.1395E+15	.1393E+15	.1391E+15	.1387E+15	.1384E+15	.1380E+15	.1373E+15
	.8170E+08	.1633E+09	.4081E+09	.8156E+09	.1630E+10	.4069E+10	.8125E+10	.1622E+11	.4043E+11
0(EV)	.3768E+00	.3913E+00	.4265E+00	.4754E+00	.5604E+00	.7844E+00	.1142E+01	.1890E+01	.4404E+01
	.1644E+15	.1647E+15	.1644E+15	.1642E+15	.1639E+15	.1635E+15	.1632E+15	.1627E+15	.1620E+15
	.9808E+08	.1961E+09	.4900E+09	.9795E+09	.1958E+10	.4888E+10	.9763E+10	.1944E+11	.4860E+11

Table III B

Medium Density Rosseland Opacity [cm^2/g], Energy [erg/g], Pressure [dyn/cm^2]

for X = 0.770, Y = 0.212, Z = 0.018

T/RHO	1.0000E-03	2.0000E-03	5.0000E-03	1.0000E-02	2.0000E-02	5.0000E-02	1.0000E-01	2.0000E-01	5.0000E-01
.06(EV)	.5398E+05	.7600E+05	0.	0.	0.	0.	0.	0.	0.
	.2497E+14	.2407E+14	0.	0.	0.	0.	0.	0.	0.
	.8581E+10	.1665E+11	0.	0.	0.	0.	0.	0.	0.
.00(EV)	.2400E+05	.3371E+05	.4900E+05	.6200E+05	0.	0.	0.	0.	0.
	.3081E+14	.2984E+14	.2839E+14	.2712E+14	0.	0.	0.	0.	0.
	.1107E+11	.2320E+11	.5589E+11	.1079E+12	0.	0.	0.	0.	0.
.00(EV)	.1172E+05	.1670E+05	.2504E+05	.3200E+05	.3806E+05	0.	0.	0.	0.
	.3691E+14	.3579E+14	.3409E+14	.3265E+14	.3109E+14	0.	0.	0.	0.
	.1521E+11	.2985E+11	.7214E+11	.1397E+12	.2692E+12	0.	0.	0.	0.
.50(EV)	.4482E+04	.6788E+04	.1072E+05	.1402E+05	.1700E+05	0.	0.	0.	0.
	.4389E+14	.4293E+14	.4124E+14	.3959E+14	.3781E+14	0.	0.	0.	0.
	.1937E+11	.3818E+11	.9283E+11	.1801E+12	.3483E+12	0.	0.	0.	0.
.00(EV)	.2003E+04	.2962E+04	.4703E+04	.6444E+04	.8385E+04	0.	0.	0.	0.
	.5034E+14	.4952E+14	.4802E+14	.4634E+14	.4446E+14	0.	0.	0.	0.
	.2347E+11	.4643E+11	.1135E+12	.2209E+12	.4284E+12	0.	0.	0.	0.
.00(EV)	.5888E+03	.8823E+03	.1395E+04	.1907E+04	.2594E+04	.3913E+04	.5100E+04	0.	0.
	.6280E+14	.6214E+14	.6085E+14	.5930E+14	.5735E+14	.5492E+14	.5387E+14	0.	0.
	.3163E+11	.6284E+11	.1548E+12	.3031E+12	.5905E+12	.1439E+13	.2870E+13	0.	0.
.00(EV)	.2436E+03	.3748E+03	.6002E+03	.8200E+03	.1118E+04	.1702E+04	.2300E+04	0.	0.
	.7507E+14	.7447E+14	.7332E+14	.7186E+14	.6988E+14	.6769E+14	.6660E+14	0.	0.
	.3975E+11	.7911E+11	.1957E+12	.3852E+12	.7533E+12	.1850E+13	.3694E+13	0.	0.
.00(EV)	.1211E+03	.1941E+03	.3234E+03	.4431E+03	.6004E+03	.9097E+03	.1241E+04	.1700E+04	0.
	.8732E+14	.8668E+14	.8567E+14	.8424E+14	.8228E+14	.7988E+14	.7898E+14	.7838E+14	0.
	.4788E+11	.9531E+11	.2366E+12	.4672E+12	.9160E+12	.2294E+13	.4504E+13	.9057E+13	0.
.00(EV)	.4354E+02	.7494E+02	.1322E+03	.1878E+03	.2597E+03	.3910E+03	.5336E+03	.7199E+03	.1100E+04
	.1119E+15	.1111E+15	.1102E+15	.1090E+15	.1070E+15	.1040E+15	.1028E+15	.1022E+15	.1007E+15
	.6418E+11	.1277E+12	.3179E+12	.6312E+12	.1244E+13	.3042E+13	.6075E+13	.1221E+14	.3059E+14
.00(EV)	.1826E+02	.3423E+02	.6957E+02	.1060E+03	.1517E+03	.2259E+03	.3063E+03	.4221E+03	.6302E+03
	.1365E+15	.1356E+15	.1345E+15	.1336E+15	.1318E+15	.1283E+15	.1265E+15	.1259E+15	.1245E+15
	.8053E+11	.1603E+12	.3988E+12	.7946E+12	.1572E+13	.3850E+13	.7646E+13	.1537E+14	.3853E+14
.00(EV)	.8821E+01	.1722E+02	.3800E+02	.6350E+02	.9617E+02	.1504E+03	.2075E+03	.2845E+03	.4225E+03
	.1614E+15	.1606E+15	.1589E+15	.1580E+15	.1565E+15	.1529E+15	.1504E+15	.1494E+15	.1482E+15
	.9703E+11	.1934E+12	.4797E+12	.9569E+12	.1901E+13	.4667E+13	.9233E+13	.1849E+14	.4646E+14
.00(EV)	.2981E+01	.5805E+01	.1415E+02	.2596E+02	.4369E+02	.7634E+02	.1109E+03	.1574E+03	.2347E+03
	.2104E+15	.2101E+15	.2083E+15	.2069E+15	.2057E+15	.2022E+15	.1993E+15	.1975E+15	.1944E+15
	.1297E+12	.2509E+12	.6432E+12	.1281E+13	.2554E+13	.6302E+13	.1249E+14	.2491E+14	.6253E+14
.00(EV)	.1579E+01	.2784E+01	.6484E+01	.1236E+02	.2244E+02	.4366E+02	.6730E+02	.1004E+03	.1574E+03
	.2603E+15	.2595E+15	.2578E+15	.2560E+15	.2548E+15	.2514E+15	.2484E+15	.2467E+15	.2449E+15
	.1684E+12	.3243E+12	.8073E+12	.1606E+13	.3206E+13	.7937E+13	.1575E+14	.3144E+14	.7870E+14
.00(EV)	.1021E+01	.1611E+01	.3447E+01	.6579E+01	.1245E+02	.2611E+02	.4194E+02	.6512E+02	.1004E+03
	.3226E+15	.3220E+15	.3208E+15	.3196E+15	.3177E+15	.3150E+15	.3133E+15	.3113E+15	.3070E+15
	.2037E+12	.4071E+12	.1016E+13	.2020E+13	.4040E+13	.1005E+14	.2006E+14	.3992E+14	.9922E+14
.00(EV)	.7665E+00	.1094E+01	.2096E+01	.3791E+01	.7192E+01	.1577E+02	.2507E+02	.3830E+02	.6400E+02
	.3842E+15	.3836E+15	.3824E+15	.3812E+15	.3796E+15	.3766E+15	.3750E+15	.3720E+15	.3683E+15
	.2447E+12	.4890E+12	.1220E+13	.2437E+13	.4862E+13	.1209E+14	.2416E+14	.4812E+14	.1194E+15
.00(EV)	.5400E+00	.6906E+00	.1102E+01	.1746E+01	.3013E+01	.6459E+01	.1086E+02	.1685E+02	.2784E+02
	.5073E+15	.5067E+15	.5055E+15	.5043E+15	.5028E+15	.5002E+15	.4981E+15	.4958E+15	.4915E+15
	.3266E+12	.6527E+12	.1630E+13	.3256E+13	.6500E+13	.1620E+14	.3234E+14	.6453E+14	.1602E+15
.00(EV)	.4383E+00	.4985E+00	.6945E+00	.1004E+01	.1597E+01	.3215E+01	.5348E+01	.8095E+01	.1284E+02
	.6303E+15	.6297E+15	.6285E+15	.6274E+15	.6259E+15	.6233E+15	.6215E+15	.6188E+15	.6141E+15
	.4084E+12	.8164E+12	.2039E+13	.4074E+13	.8137E+13	.2030E+14	.4054E+14	.8094E+14	.2011E+15
.00(EV)	.3982E+00	.4226E+00	.5165E+00	.6618E+00	.9378E+00	.1728E+01	.2829E+01	.4388E+01	.7009E+01
	.7832E+15	.7526E+15	.7514E+15	.7503E+15	.7488E+15	.7461E+15	.7443E+15	.7419E+15	.7370E+15
	.4982E+12	.9801E+12	.2448E+13	.4893E+13	.9775E+13	.2438E+14	.4871E+14	.9730E+14	.2481E+15
.00(EV)	.3817E+00	.3720E+00	.3996E+00	.4409E+00	.5103E+00	.7348E+00	.1059E+01	.1580E+01	.2615E+01
	.9009E+15	.9983E+15	.9972E+15	.9961E+15	.9946E+15	.9922E+15	.9900E+15	.9875E+15	.9829E+15
	.6540E+12	.1308E+13	.3267E+13	.6530E+13	.1305E+14	.3258E+14	.6509E+14	.1300E+15	.3241E+15

Table III C

High Density Rosseland Opacity [cm^2/g], Energy [erg/g], Pressure [dyn/cm^2]

for X = 0.770, Y = 0.212, Z = 0.018

RT/RHO	1.0000E+00	2.0000E+00	5.0000E+00	1.0000E+01	2.0000E+01	5.0000E+01	1.0000E+02	2.0000E+02
50.00(EV)	.8600E+03	0.	0.	0.	0.	0.	0.	0.
	.1229E+15	0.	0.	0.	0.	0.	0.	0.
	.7709E+14	0.	0.	0.	0.	0.	0.	0.
60.00(EV)	.5657E+03	0.	0.	0.	0.	0.	0.	0.
	.1469E+15	0.	0.	0.	0.	0.	0.	0.
	.9314E+14	0.	0.	0.	0.	0.	0.	0.
80.00(EV)	.3088E+03	.4114E+03	0.	0.	0.	0.	0.	0.
	.1952E+15	.1938E+15	0.	0.	0.	0.	0.	0.
	.1254E+15	.2516E+15	0.	0.	0.	0.	0.	0.
00.00(EV)	.1994E+03	.2477E+03	0.	0.	0.	0.	0.	0.
	.2438E+15	.2429E+15	0.	0.	0.	0.	0.	0.
	.1578E+15	.3166E+15	0.	0.	0.	0.	0.	0.
25.00(EV)	.1263E+03	.1573E+03	.2163E+03	0.	0.	0.	0.	0.
	.9040E+15	.3022E+15	.3001E+15	0.	0.	0.	0.	0.
	.1982E+15	.3966E+15	.9968E+15	0.	0.	0.	0.	0.
50.00(EV)	.8693E+02	.1058E+03	.1339E+03	0.	0.	0.	0.	0.
	.3650E+15	.3624E+15	.3606E+15	0.	0.	0.	0.	0.
	.2387E+15	.4777E+15	.1199E+16	0.	0.	0.	0.	0.
00.00(EV)	.3601E+02	.4407E+02	.5886E+02	.7430E+02	0.	0.	0.	0.
	.4881E+15	.4844E+15	.4812E+15	.4804E+15	0.	0.	0.	0.
	.3201E+15	.6405E+15	.1602E+16	.3225E+16	0.	0.	0.	0.
50.00(EV)	.1726E+02	.2182E+02	.2932E+02	.3764E+02	0.	0.	0.	0.
	.6185E+15	.6073E+15	.6025E+15	.6008E+15	0.	0.	0.	0.
	.4809E+15	.8033E+15	.2008E+16	.4030E+16	0.	0.	0.	0.
00.00(EV)	.9460E+01	.1224E+02	.1704E+02	.2200E+02	0.	0.	0.	0.
	.7331E+15	.7295E+15	.7244E+15	.7218E+15	0.	0.	0.	0.
	.4822E+15	.9650E+15	.2415F+16	.4838E+16	0.	0.	0.	0.
00.00(EV)	.3615E+01	.4790E+01	.6784F+01	.8854E+01	.1171E+02	.1741E+02	.2501E+02	0.
	.9788E+15	.9750E+15	.9687E+15	.9649E+15	.9637E+15	.9774E+15	.1010E+16	0.
	.6460E+15	.1290E+16	.3229E+16	.6462E+16	.1298E+17	.3319E+17	.6911E+17	0.
00.00(EV)	.1786E+01	.2421E+01	.3442E+01	.4503E+01	.6030E+01	.9186E+01	.1299E+02	.1881E+02
	.1324E+16	.1220E+16	.1214F+16	.1209E+16	.1206E+16	.1215E+16	.1244E+16	.1305E+16
	.8698E+15	.1615E+16	.4041E+16	.8092E+16	.1622E+17	.4114E+17	.8477E+17	.1790E+18
00.00(EV)	.1061E+01	.1417E+01	.2046E+01	.2692E+01	.3572E+01	.5355F+01	.7728E+01	.1100E+02
	.1469E+16	.1465E+16	.1459F+16	.1453E+16	.1450E+16	.1459E+16	.1480E+16	.1538E+16
	.9737E+15	.1941E+16	.4852F+16	.9721E+16	.1947E+17	.4915E+17	.1005E+18	.2102E+18
00.00(EV)	.5928E+00	.7384E+00	.1023F+01	.1329E+01	.1742E+01	.2585E+01	.3803E+01	.5092E+01
	.1980E+16	.1955E+16	.1949F+16	.1943E+16	.1938E+16	.1939E+16	.1956E+16	.2007E+16
	.1302E+16	.2598E+16	.6474F+16	.1297E+17	.2599E+17	.6529E+17	.1324E+18	.2730E+18
00.00(EV)	.4678E+00	.5818E+00	.6975F+00	.8774E+00	.1173E+01	.1590E+01	.2169E+01	.3014E+01
	.2452E+16	.2444E+16	.2439F+16	.2433E+16	.2427E+16	.2429F+16	.2437E+16	.2480E+16
	.1629E+16	.3253E+16	.8104F+16	.1621E+17	.3251E+17	.8154E+17	.1645E+18	.3362E+18
0.00(EV)	.9E+00	.4633E+00	.5513F+00	.6566E+00	.8080E+00	.1081F+01	.1399E+01	.1865E+01
	.1E+16	.3060E+16	.3052E+16	.3046E+16	.3034E+16	.3075E+16	.3044E+16	.3073E+16
	.2E+16	.4072E+16	.1015F+17	.2027E+17	.4064E+17	.1019E+18	.2049E+18	.4155E+18
0.00(EV)	.3851E+00	.4199E+00	.4826F+00	.5515E+00	.6510E+00	.8344E+00	.1028E+01	.1308E+01
	.3680E+16	.3674E+16	.3664E+16	.3659E+16	.3652E+16	.3646E+16	.3642E+16	.3678E+16
	.2447E+16	.4891E+16	.1220E+17	.2434E+17	.4875E+17	.1223E+18	.2455E+18	.4961E+18

Table IV A

Low Density Rosseland Opacity [cm^2/g], Energy [erg/g], Pressure [dyn/cm^2]

for X = 0.8832, Y = 0.1150, Z = 0.0018

KT/RHO	1.0000E-06	2.0000E-06	5.0000E-06	1.0000E-05	2.0000E-05	5.0000E-05	1.0000E-04	2.0000E-04	5.0000E-04
1.00(EV)	.7958E+03	.8523E+03	.1043E+04	.1221E+04	.1441E+04	0.	0.	0.	0.
	.4522E+13	.4226E+13	.3955E+13	.3814E+13	.3714E+13	0.	0.	0.	0.
	.9406E+06	.1842E+07	.4519E+07	.8952E+07	.1778E+08	0.	0.	0.	0.
1.25(EV)	.2769E+04	.3450E+04	.4427E+04	.5259E+04	.6200E+04	.7698E+04	.9100E+04	0.	0.
	.8144E+13	.7095E+13	.6036E+13	.5452E+13	.5008E+13	.4586E+13	.4373E+13	0.	0.
	.1487E+07	.2608E+07	.6301E+07	.1214E+08	.2361E+08	.5743E+08	.1132E+09	0.	0.
1.50(EV)	.4218E+04	.6334E+04	.9756E+04	.1269E+05	.1586E+05	.2047E+05	.2451E+05	.2900E+05	0.
	.1304E+14	.1150E+14	.9677E+13	.8441E+13	.7429E+13	.6396E+13	.5822E+13	.5420E+13	0.
	.2111E+07	.3943E+07	.8988E+07	.1686E+08	.3189E+08	.7504E+08	.1449E+09	.2827E+09	0.
2.00(EV)	.2744E+04	.5504E+04	.1278E+05	.2234E+05	.3591E+05	.5924E+05	.8062E+05	.1100E+06	0.
	.1004E+14	.1757E+14	.1635E+14	.1515E+14	.1378E+14	.1190E+14	.1058E+14	.9434E+13	0.
	.3275E+07	.6384E+07	.1525E+08	.2903E+08	.5475E+08	.1257E+09	.2360E+09	.4457E+09	0.
2.50(EV)	.1604E+04	.3471E+04	.9332E+04	.1890E+05	.3634E+05	.7748E+05	.1245E+06	0.	0.
	.2028E+14	.2007E+14	.1953E+14	.1894E+14	.1806E+14	.1659E+14	.1532E+14	0.	0.
	.4221E+07	.8342E+07	.2043E+08	.3999E+08	.7728E+08	.1878E+09	.3470E+09	0.	0.
3.00(EV)	.1067E+04	.2351E+04	.6569E+04	.1399E+05	.2904E+05	.6948E+05	.1140E+06	.1699E+06	.3100E+06
	.2178E+14	.2170E+14	.2145E+14	.2111E+14	.2064E+14	.1967E+14	.1848E+14	.1751E+14	.1576E+14
	.5116E+07	.1017E+08	.2507E+08	.4953E+08	.9750E+08	.2350E+09	.4531E+09	.8679E+09	.2019E+10
4.00(EV)	.5062E+03	.1051E+04	.2740E+04	.5570E+04	.1134E+05	.2751E+05	.5002E+05	.8468E+05	.1500E+06
	.2458E+14	.2448E+14	.2430E+14	.2412E+14	.2392E+14	.2348E+14	.2295E+14	.2220E+14	.2101E+14
	.6886E+07	.1364E+08	.3391E+08	.6726E+08	.1337E+09	.3290E+09	.6452E+09	.1261E+10	.3013E+10
5.00(EV)	.2048E+03	.4206E+03	.1065E+04	.2110E+04	.4109E+04	.9462E+04	.1693E+05	.2970E+05	.5793E+05
	.2885E+14	.2769E+14	.2728E+14	.2699E+14	.2672E+14	.2636E+14	.2600E+14	.2555E+14	.2465E+14
	.8694E+07	.1727E+08	.4277E+08	.8488E+08	.1684E+09	.4164E+09	.8244E+09	.1630E+10	.3947E+10
6.00(EV)	.8201E+02	.1750E+03	.4622E+03	.9341E+03	.1845E+04	.4331E+04	.8067E+04	.1425E+05	.2707E+05
	.3133E+14	.3114E+14	.3072E+14	.3031E+14	.2987E+14	.2932E+14	.2893E+14	.2859E+14	.2772E+14
	.1052E+08	.2095E+08	.5190E+08	.1029E+09	.2041E+09	.5046E+09	.1001E+10	.1978E+10	.4847E+10
8.00(EV)	.2249E+02	.4700E+02	.1290E+03	.2712E+03	.5599E+03	.1413E+04	.2761E+04	.5201E+04	.1085E+05
	.3662E+14	.3674E+14	.3658E+14	.3634E+14	.3614E+14	.3563E+14	.3514E+14	.3464E+14	.3374E+14
	.1408E+08	.2810E+08	.6995E+08	.1392E+09	.2771E+09	.6853E+09	.1358E+10	.2697E+10	.6636E+10
10.00(EV)	.9971E+01	.2002E+02	.5194E+02	.1081E+03	.2224E+03	.5584E+03	.1091E+04	.2044E+04	.4410E+04
	.4218E+14	.4208E+14	.4195E+14	.4174E+14	.4161E+14	.4126E+14	.4087E+14	.4048E+14	.3975E+14
	.1764E+08	.3520E+08	.8773E+08	.1748E+09	.3488E+09	.8642E+09	.1714E+10	.3409E+10	.8434E+10
12.50(EV)	.4203E+01	.8101E+01	.2015E+02	.4031E+02	.7996E+02	.1902E+03	.3522E+03	.6362E+03	.1335E+04
	.4885E+14	.4876E+14	.4864E+14	.4850E+14	.4832E+14	.4800E+14	.4762E+14	.4725E+14	.4674E+14
	.2207E+08	.4408E+08	.1100E+09	.2194E+09	.4372E+09	.1086E+10	.2157E+10	.4288E+10	.1066E+11
15.00(EV)	.1904E+01	.3476E+01	.8039E+01	.1571E+02	.3059E+02	.7140E+02	.1313E+03	.2340E+03	.4808E+03
	.5552E+14	.5543E+14	.5529E+14	.5516E+14	.5499E+14	.5463E+14	.5430E+14	.5406E+14	.5346E+14
	.2651E+08	.5296E+08	.1321E+09	.2637E+09	.5260E+09	.1307E+10	.2604E+10	.5188E+10	.1287E+11
20.00(EV)	.8215E+00	.1173E+01	.2141E+01	.3726E+01	.6882E+01	.1491E+02	.2941E+02	.5269E+02	.1070E+03
	.6865E+14	.6877E+14	.6862E+14	.6849E+14	.6833E+14	.6804E+14	.6775E+14	.6730E+14	.6677E+14
	.3539E+08	.7072E+08	.1765E+09	.3529E+09	.7038E+09	.1753E+10	.3495E+10	.6960E+10	.1724E+11
25.00(EV)	.5696E+00	.7067E+00	.1054E+01	.1577E+01	.2596E+01	.5600E+01	.1021E+02	.1844E+02	.3870E+02
	.8216E+14	.8209E+14	.8195E+14	.8182E+14	.8164E+14	.8134E+14	.8104E+14	.8066E+14	.8004E+14
	.4426E+08	.8846E+08	.2209E+09	.4413E+09	.8812E+09	.2197E+10	.4381E+10	.8731E+10	.2170E+11
30.00(EV)	.4770E+00	.5470E+00	.7160E+00	.9537E+00	.1392E+01	.2644E+01	.4729E+01	.8677E+01	.1824E+02
	.9550E+14	.9542E+14	.9528E+14	.9514E+14	.9498E+14	.9465E+14	.9434E+14	.9395E+14	.9332E+14
	.5314E+08	.1062E+09	.2653E+09	.5301E+09	.1054E+10	.2640E+10	.5247E+10	.1050E+11	.2613E+11
40.00(EV)	.4087E+00	.4316E+00	.4906E+00	.5714E+00	.7117E+00	.1101E+01	.1743E+01	.2996E+01	.6372E+01
	.1222E+15	.1221E+15	.1219E+15	.1218E+15	.1216E+15	.1213E+15	.1211E+15	.1208E+15	.1199E+15
	.7084E+08	.1417E+09	.3540E+09	.7076E+09	.1414E+10	.3529E+10	.7047E+10	.1405E+11	.3497E+11
50.00(EV)	.3914E+00	.4031E+00	.4301E+00	.4660E+00	.5298E+00	.6930E+00	.9411E+00	.1429E+01	.2844E+01
	.1488E+15	.1487E+15	.1486E+15	.1485E+15	.1483E+15	.1480E+15	.1477E+15	.1473E+15	.1466E+15
	.8864E+08	.1772E+09	.4428E+09	.8851E+09	.1769E+10	.4416E+10	.8820E+10	.1761E+11	.4384E+11
60.00(EV)	.3849E+00	.3910E+00	.4058E+00	.4241E+00	.4601E+00	.5472E+00	.6747E+00	.9124E+00	.1618E+01
	.1755E+15	.1754E+15	.1753E+15	.1751E+15	.1749E+15	.1746E+15	.1743E+15	.1739E+15	.1732E+15
	.1064E+09	.2127E+09	.5316E+09	.1062E+10	.2124E+10	.5304E+10	.1060E+11	.2118E+11	.5275E+11

Table IV B

Medium Density Rosseland Opacity [cm^2/g], Energy [erg/g], Pressure [dyn/cm^2]

for X = 0.8832, Y = 0.1150, Z = 0.0018

KT/RHO	1.0000E-03	2.0000E-03	5.0000E-03	1.0000E-02	2.0000E-02	5.0000E-02	1.0000E-01	2.0000E-01	5.0000E-01
6.00(EV)	.4123E+05	.5900E+05	0.	0.	0.	0.	0.	0.	0.
	.2692E+14	.2593E+14	0.	0.	0.	0.	0.	0.	0.
	.9454E+10	.1835E+11	0.	0.	0.	0.	0.	0.	0.
8.00(EV)	.1666E+05	.2339E+05	.3400E+05	.4300E+05	0.	0.	0.	0.	0.
	.3293E+14	.3200E+14	.3050E+14	.2913E+14	0.	0.	0.	0.	0.
	.1304E+11	.2551E+11	.6145E+11	.1186E+12	0.	0.	0.	0.	0.
10.00(EV)	.7178E+04	.1031E+05	.1570E+05	.2000E+05	.2400E+05	0.	0.	0.	0.
	.3894E+14	.3796E+14	.3636E+14	.3491E+14	.3329E+14	0.	0.	0.	0.
	.1663E+11	.3264E+11	.7908E+11	.1532E+12	.2954E+12	0.	0.	0.	0.
12.50(EV)	.2214E+04	.3529E+04	.5919E+04	.8058E+04	.1000E+05	0.	0.	0.	0.
	.4606E+14	.4520E+14	.4360E+14	.4201E+14	.4027E+14	0.	0.	0.	0.
	.2110E+11	.4135E+11	.1013E+12	.1960E+12	.3812E+12	0.	0.	0.	0.
15.00(EV)	.7931E+03	.1284E+04	.2331E+04	.3391E+04	.4756E+04	0.	0.	0.	0.
	.5287E+14	.5210E+14	.5062E+14	.4897E+14	.4716E+14	0.	0.	0.	0.
	.2553E+11	.5054E+11	.1237E+12	.2407E+12	.4678E+12	0.	0.	0.	0.
20.00(EV)	.1770E+03	.2892E+03	.5366E+03	.8370E+03	.1293E+04	.2238E+04	.3100E+04	0.	0.
	.6623E+14	.6557E+14	.6426E+14	.6264E+14	.6067E+14	.5845E+14	.5776E+14	0.	0.
	.3437E+11	.6831E+11	.1682E+12	.3294E+12	.6428E+12	.1572E+13	.3151E+13	0.	0.
25.00(EV)	.6410E+02	.1034E+03	.1919E+03	.3023E+03	.4821E+03	.8745E+03	.1300E+04	0.	0.
	.7946E+14	.7885E+14	.7766E+14	.7611E+14	.7404E+14	.7204E+14	.7125E+14	0.	0.
	.4318E+11	.8595E+11	.2127E+12	.4184E+12	.8181E+12	.2017E+13	.4041E+13	0.	0.
30.00(EV)	.3035E+02	.4912E+02	.9054E+02	.1418E+03	.2260E+03	.4173E+03	.6373E+03	.9300E+03	0.
	.9269E+14	.9204E+14	.9099E+14	.8950E+14	.8737E+14	.8506E+14	.8449E+14	.8425E+14	0.
	.5199E+11	.1038E+12	.2570E+12	.5074E+12	.9941E+12	.2447E+13	.4919E+13	.9923E+13	0.
40.00(EV)	.1064E+02	.1803E+02	.3278E+02	.5058E+02	.7870E+02	.1434E+03	.2226E+03	.3379E+03	.6200E+03
	.1192E+15	.1184E+15	.1175E+15	.1162E+15	.1140E+15	.1108E+15	.1100E+15	.1097E+15	.1085E+15
	.6968E+11	.1387E+12	.3453E+12	.6852E+12	.1349E+13	.3303E+13	.6617E+13	.1334E+14	.3348E+14
50.00(EV)	.4971E+01	.8546E+01	.1652E+02	.2587E+02	.3925E+02	.6904E+02	.1062E+03	.1628E+03	.2957E+03
	.1458E+15	.1444E+15	.1438E+15	.1428E+15	.1408E+15	.1371E+15	.1355E+15	.1353E+15	.1342E+15
	.8741E+11	.1740E+12	.4331E+12	.8627E+12	.1706E+13	.4176E+13	.8313E+13	.1675E+14	.4210E+14
60.00(EV)	.2916E+01	.4651E+01	.9247E+01	.1497E+02	.2308E+02	.4025E+02	.6197E+02	.9386E+02	.1692E+03
	.1727E+15	.1719E+15	.1702E+15	.1692E+15	.1675E+15	.1634E+15	.1611E+15	.1600E+15	.1598E+15
	.1053E+12	.2094E+12	.5208E+12	.1039E+13	.2063E+13	.5061E+13	.1003E+14	.2014E+14	.5072E+14
80.00(EV)	.1207E+01	.1928E+01	.3811E+01	.6379E+01	.1033E+02	.1825E+02	.2801E+02	.4247E+02	.7231E+02
	.2259E+15	.2252E+15	.2233E+15	.2220E+15	.2207E+15	.2169E+15	.2148E+15	.2129E+15	.2118E+15
	.1407E+12	.2810E+12	.6979E+12	.1391E+13	.2772E+13	.6836E+13	.1355E+14	.2700E+14	.6812E+14
100.00(EV)	.7774E+00	.1112E+01	.2026E+01	.3377E+01	.5625E+01	.1041E+02	.1598E+02	.2408E+02	.3957E+02
	.2791E+15	.2784E+15	.2767E+15	.2749E+15	.2737E+15	.2701E+15	.2671E+15	.2656E+15	.2644E+15
	.1762E+12	.3518E+12	.8758E+12	.1743E+13	.3474E+13	.8608E+13	.1709E+14	.3417E+14	.8570E+14
125.00(EV)	.5952E+00	.7624E+00	.1220E+01	.1921E+01	.3134E+01	.5854E+01	.9078E+01	.1360E+02	.2161E+02
	.3463E+15	.3457E+15	.3446E+15	.3434E+15	.3415E+15	.3389E+15	.3374E+15	.3353E+15	.3314E+15
	.2210E+12	.4415E+12	.1102E+13	.2200E+13	.4382E+13	.1090E+14	.2177E+14	.4334E+14	.1079E+15
150.00(EV)	.5073E+00	.6027E+00	.8613E+00	.1252E+01	.1969E+01	.3478E+01	.5343E+01	.7731E+01	.1270E+02
	.4129E+15	.4123E+15	.4111E+15	.4100E+15	.4083E+15	.4053E+15	.4039E+15	.4018E+15	.3975E+15
	.2693E+12	.5303E+12	.1324E+13	.2643E+13	.5277E+13	.1312E+14	.2622E+14	.5224E+14	.1298E+15
200.00(EV)	.4289E+00	.4696E+00	.5716E+00	.7204E+00	.9890E+00	.1634E+01	.2383E+01	.3376E+01	.5267E+01
	.5461E+15	.5455E+15	.5443E+15	.5431E+15	.5415E+15	.5389E+15	.5364E+15	.5340E+15	.5304E+15
	.3541E+12	.7078E+12	.1767E+13	.3530E+13	.7049E+13	.1757E+14	.3500E+14	.7001E+14	.1740E+15
250.00(EV)	.3968E+00	.4149E+00	.4633E+00	.5327E+00	.6546E+00	.9522E+00	.1313E+01	.1779E+01	.2575E+01
	.6763E+15	.6786E+15	.6775E+15	.6760E+15	.6747E+15	.6721E+15	.6703E+15	.6676E+15	.6632E+15
	.4418E+12	.8853E+12	.2211E+13	.4418E+13	.8823E+13	.2201E+14	.4397E+14	.8778E+14	.2182E+15
300.00(EV)	.3847E+00	.3947E+00	.4218E+00	.4574E+00	.5179E+00	.6710E+00	.8670E+00	.1142E+01	.1667E+01
	.8124E+15	.8110E+15	.8106E+15	.8095E+15	.8079E+15	.8050E+15	.8033E+15	.8008E+15	.7960E+15
	.5316E+12	.1060E+13	.2659E+13	.5306E+13	.1060E+14	.2644E+14	.5284E+14	.1059E+15	.2624E+15
400.00(EV)	.3786E+00	.3792E+00	.3883E+00	.4011E+00	.4225E+00	.4749E+00	.5495E+00	.6616E+00	.8948E+00
	.1019E+16	.1071E+16	.1077E+16	.1074E+16	.1074E+16	.1072E+16	.1069E+16	.1067E+16	.1042E+16
	.7091E+12	.1416E+13	.3542E+13	.7080E+13	.1415E+14	.3533E+14	.7056E+14	.1410E+15	.3516E+15

Table IV C

High Density Rosseland Opacity [cm^2/g], Energy [erg/g], Pressure [dyn/cm^2]

for X = 0.8832, Y = 0.1150, Z = 0.0018

T/RHO	1.0000E-00	2.0000E-00	5.0000E-00	1.0000E-01	2.0000E-01	5.0000E-01	1.0000E-02	2.0000E-02
).00(EV)	.4800E+03	0.	0.	0.	0.	0.	0.	0.
	.1326E+15	0.	0.	0.	0.	0.	0.	0.
	.0420E+14	0.	0.	0.	0.	0.	0.	0.
).00(EV)	.2697E+03	0.	0.	0.	0.	0.	0.	0.
	.1586E+15	0.	0.	0.	0.	0.	0.	0.
	.1817E+15	0.	0.	0.	0.	0.	0.	0.
).00(EV)	.1103E+03	.1730E+03	0.	0.	0.	0.	0.	0.
	.2105E+15	.2090E+15	0.	0.	0.	0.	0.	0.
	.1366E+15	.2740E+15	0.	0.	0.	0.	0.	0.
).00(EV)	.5615E+02	.8329E+02	0.	0.	0.	0.	0.	0.
	.2630E+15	.2612E+15	0.	0.	0.	0.	0.	0.
	.1717E+15	.3440E+15	0.	0.	0.	0.	0.	0.
).00(EV)	.2958E+02	.4254E+02	0.	0.	0.	0.	0.	0.
	.3285E+15	.3262E+15	0.	0.	0.	0.	0.	0.
	.2157E+15	.4317E+15	0.	0.	0.	0.	0.	0.
).00(EV)	.1795E+02	.2499E+02	.4289E+02	0.	0.	0.	0.	0.
	.3944E+15	.3918E+15	.3893E+15	0.	0.	0.	0.	0.
	.2597E+15	.5191E+15	.1303E+16	0.	0.	0.	0.	0.
).00(EV)	.7119E+01	.9933E+01	.1721E+02	0.	0.	0.	0.	0.
	.5271E+15	.5236E+15	.5199E+15	0.	0.	0.	0.	0.
	.3477E+15	.6956E+15	.1740E+16	0.	0.	0.	0.	0.
).00(EV)	.3667E+01	.5081E+01	.8542E+01	.1349E+02	0.	0.	0.	0.
	.6536E+15	.6560E+15	.6512E+15	.6499E+15	0.	0.	0.	0.
	.4384E+15	.8720E+15	.2179E+16	.4377E+16	0.	0.	0.	0.
).00(EV)	.2251E+01	.3083E+01	.5035E+01	.7753E+01	0.	0.	0.	0.
	.7923E+15	.7884E+15	.7830E+15	.7801E+15	0.	0.	0.	0.
	.5234E+15	.1048E+16	.2621E+16	.5259E+16	0.	0.	0.	0.
).00(EV)	.1149E+01	.1515E+01	.2323E+01	.3384E+01	.5235E+01	.9912E+01	.16 7E+02	0.
	.1698E+16	.1054E+16	.1048E+16	.1044E+16	.1043E+16	.1060E+16	.10 .16	0.
	.7006E+15	.1394E+16	.3504E+16	.7013E+16	.1409E+17	.3610E+17	.752 E+17	0.
0.00(EV)	.7744E+00	.9772E+00	.1404E+01	.1940E+01	.2867E+01	.5183E+01	.8341E+01	0.
	.1324E+16	.1319E+16	.1313E+16	.1308E+16	.1306E+16	.1318F+16	.1351E+16	0.
	.0783E+15	.1752E+16	.4385E+16	.8779E+16	.1760E+17	.4471E+17	.9226E+17	0.
0.00(EV)	.6054E+00	.7317E+00	.9964E+00	.1327E+01	.1857E+01	.3121E+01	.4863E+01	.7844E+01
	.1509E+16	.1584E+16	.1578E+16	.1573E+16	.1570E+16	.1577E+16	.1607E+16	.1672E+16
	.1086E+16	.2106E+16	.5264E+16	.1059E+17	.2113E+17	.5338F+17	.1094E+18	.2289E+18
0.00(EV)	.4722E+00	.5323E+00	.6614E+00	.8206E+00	.1066E+01	.1630E+01	.2388E+01	.3623E+01
	.2122E+16	.2114E+16	.2109E+16	.2103E+16	.2099E+16	.2101E+16	.2122E+16	.2180E+16
	.1411E+16	.2816E+16	.7022E+16	.1407E+17	.2820E+17	.7047E+17	.1430E+18	.2970E+18
0.00(EV)	.4234E+00	.4574E+00	.5337E+00	.6275E+00	.7693E+00	.1041E+01	.1486E+01	.2140E+01
	.2654E+16	.2644E+16	.2641E+16	.2635E+16	.2629E+16	.2628E+16	.2643E+16	.2693E+16
	.1766E+16	.3528E+16	.8788E+16	.1759E+17	.3527E+17	.8847E+17	.1780E+18	.3655E+18
0.00(EV)	.3972E+00	.4175E+00	.4622E+00	.5177E+00	.6019E+00	.7800E+00	.1003E+01	.1369E+01
	.3320E+16	.3317E+16	.3305E+16	.3299E+16	.3292E+16	.3289E+16	.3301E+16	.3335E+16
	.2210E+16	.4415E+16	.1101E+17	.2194E+17	.4404E+17	.1105E+18	.2225E+18	.4613E+18
0.00(EV)	.3817E+00	.3957E+00	.4256E+00	.4604E+00	.5158E+00	.6319E+00	.7724E+00	.9931E+00
	.3986E+16	.3979E+16	.3969E+16	.3964E+16	.3957E+16	.3951E+16	.3959E+16	.3990E+16
	.2653E+16	.5303E+16	.1323E+17	.2640E+17	.5280E+17	.1326E+18	.2664E+18	.5387E+18

Table V

Opacity due to Thermal Electron Conduction [cm^2/g]

kT[eV]	$\rho[g/cm^3]$									
	.2	.5	1	2	5	10	20	50	100	200
50	98800	27100	9060	2300	691	467	128	20.7	4.87	1.12
60		36100	13000	2750	836	654	187	31.9	7.61	1.76
80		53400	20800	7490	1130	1060	338	61.5	15.3	3.59
100		69800	28200	10800	1410	1510	499	97.0	25.6	6.16
125		88800	37000	14900	3980	1970	727	155	42.6	10.6
150			45500	18700	5330	2520	957	219	62.8	16.2
200			61400	26100	7920	3000	1370	348	111	30.8
250			76300	32900	10400	4110	1850	484	165	47.8
300			90300	39500	12700	5180	1990	651	222	69.4
400				51600	17100	7200	2910	930	338	115
500				62900	21200	9100	3780	1230	464	162
600				73500	25100	10900	4610	1390	588	217
800				93100	32300	14300	6170	1950	833	319
1000					38900	17400	7620	2470	1010	423
1250					46700	21000	9320	3090	1290	549
1500					53900	24400	10900	3670	1560	640

Table VI

Summary of opacity uncertainties in % as function of radius in standard solar model.

Composition

$R/R_\odot$	Standard					Low-Z				
	A	B	C	D	Total	A	B	C	D	Total
0	10	2	6	8	14	5	2	5	4	8
.2	8	2	8	10	15	4	2	6	5	9
.4	8	2	10	12	18	4	2	8	6	11
.6	6	1	15	15	22	3	1	12	8	15
.8	5	3	20	20	29	3	4	15	12	20
.9	5	7	20	20	30	3	10	15	12	22
.95	2	10	20	20	30	1	15	15	12	24
.995	0	7	20	15	26	0	10	15	8	20

A = uncertainty due to relative metal abundance between metals.

B = uncertainty due to a 5% change in Y with Z held constant.

C = uncertainty in data (primarily photoelectric gross section).

D = uncertainty in model based on complexity of spectrum.

Fig. 1. Extinction coefficient κ_ν' [cm^2/g] vs. pnoton energy [eV] at temperature kT = 0.5 eV and $\rho = 3 \times 10^{-7} g/cm^3$. Some important molecular contributions are included. Most of the absorption lines are of atomic origin.

Fig. 2. Equal opacity contour map as a function of temperature and density for a standard solar mixture. The dotted circles indicate conditions in a standard solar model as a function of solar radius from $R/R_\odot$ = 0 to 0.995.

Fig. 3. Curve A is the per cent change in opacity of the low-Z mixture relative to the standard mixture. Curve B is the per cent change of opacity using the Allen composition of metals relative to the standard mixture which uses the Cameron composition for the metals.

Fig. 4. Extinction coefficient as a function of $u \equiv h\nu/kT$. Curves read from the bottom up correspond to conditions in a standard solar model at radii $R/R_\odot$ = 0, 0.2, 0.4, 0.6, 0.8, 0.9, 0.95, 0.995. The strong line at $u \approx 4$ in the top extinction coefficient curve is the hydrogen Lα line. The Rosseland weighting function appropriate for all extinction coefficient curves is shown at the very top.

EXTINCTION COEFFICIENTS AT KT = 0.5 eV, RHO = $3 \cdot 10^{-7}$ G/CM^3

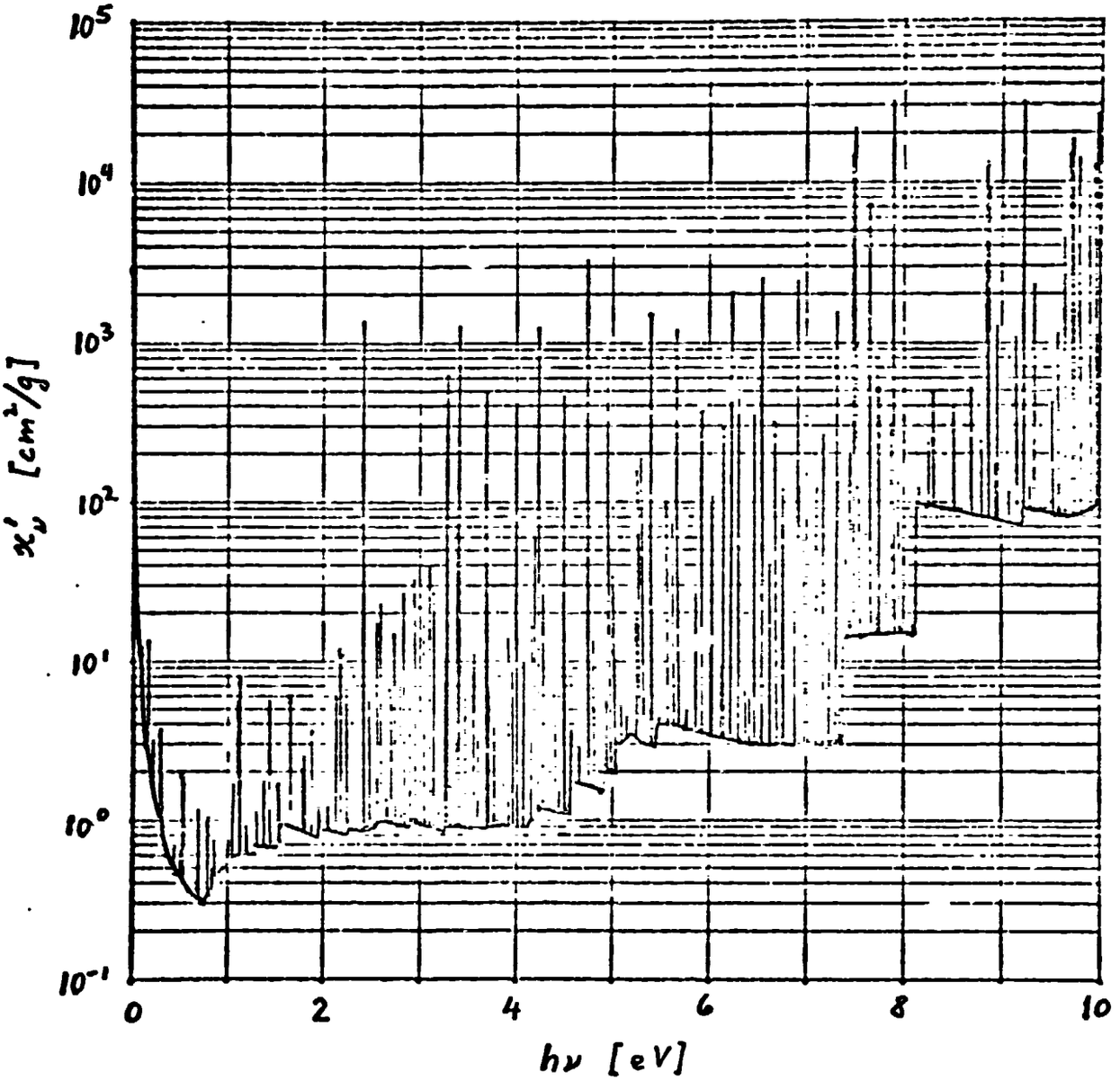

Fig. 1.

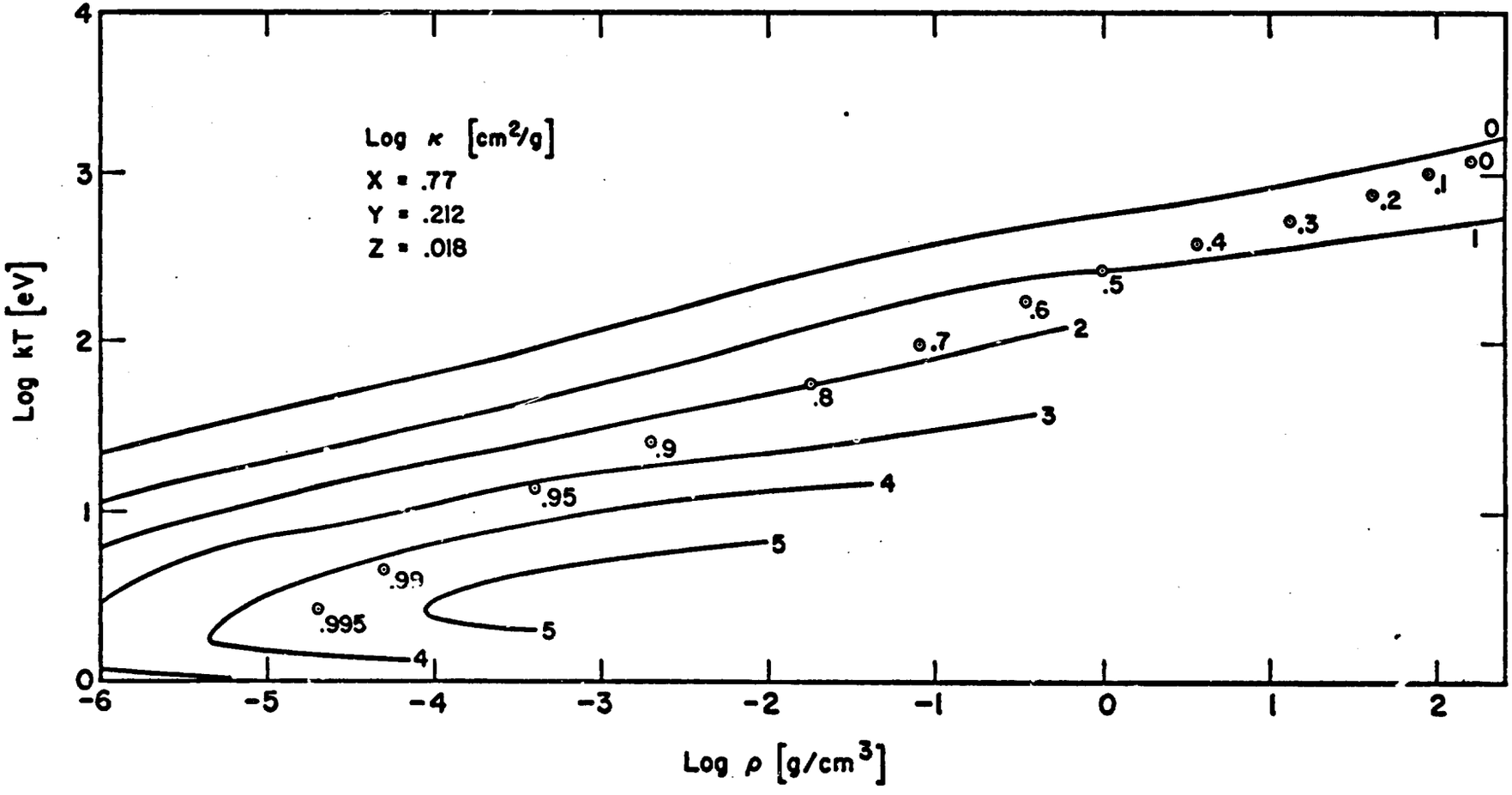
Log κ [cm²/g]
X = .77
Y = .212
Z = .018
Log kT [eV]
Log ρ [g/cm³]
0
.0
.1
.2
.3
.4
.5
.6
.7
.8
.9
.95
.99
.995
1
2
3
4
5
5
4

Fig. 2

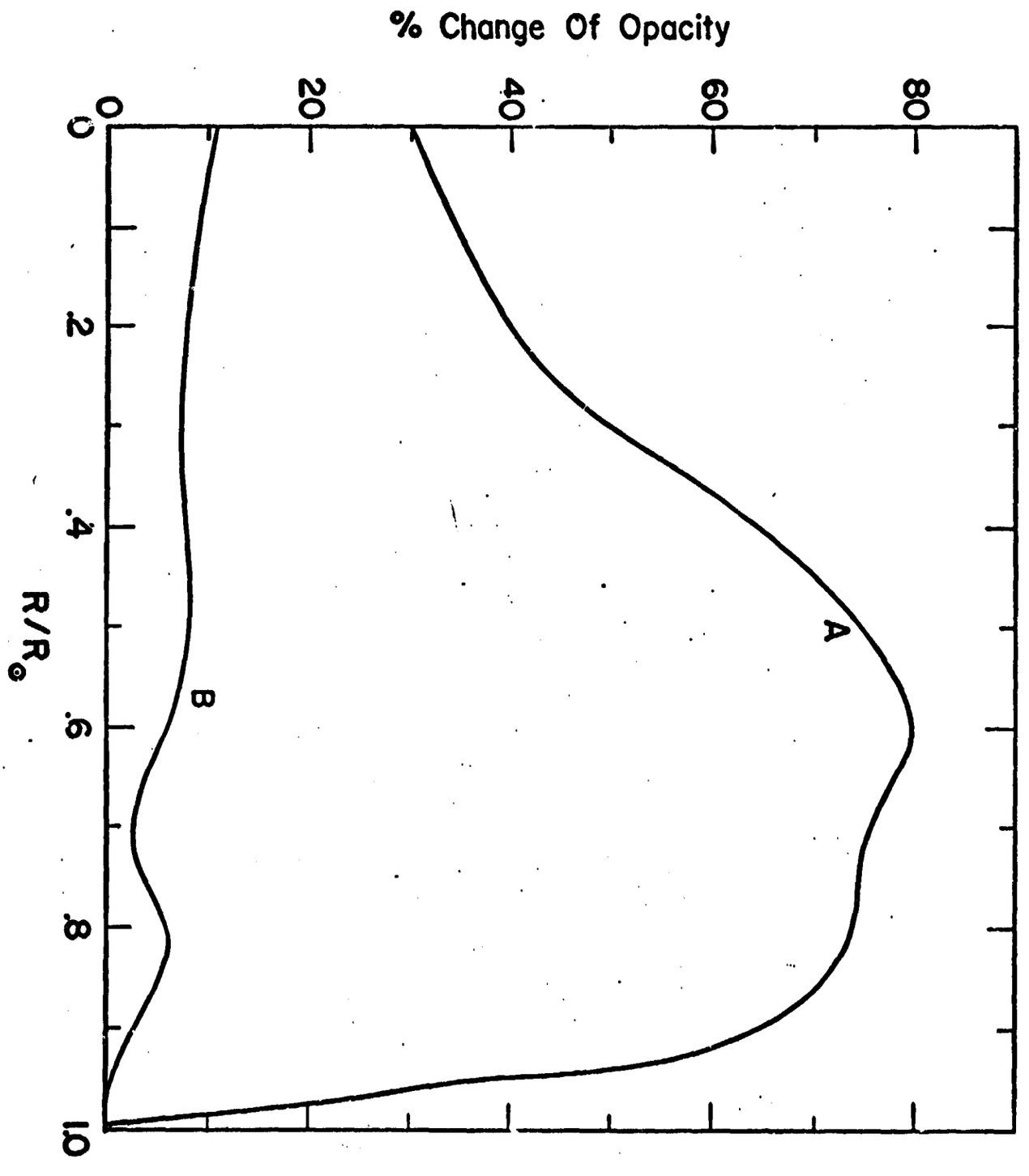

Fig. 3.

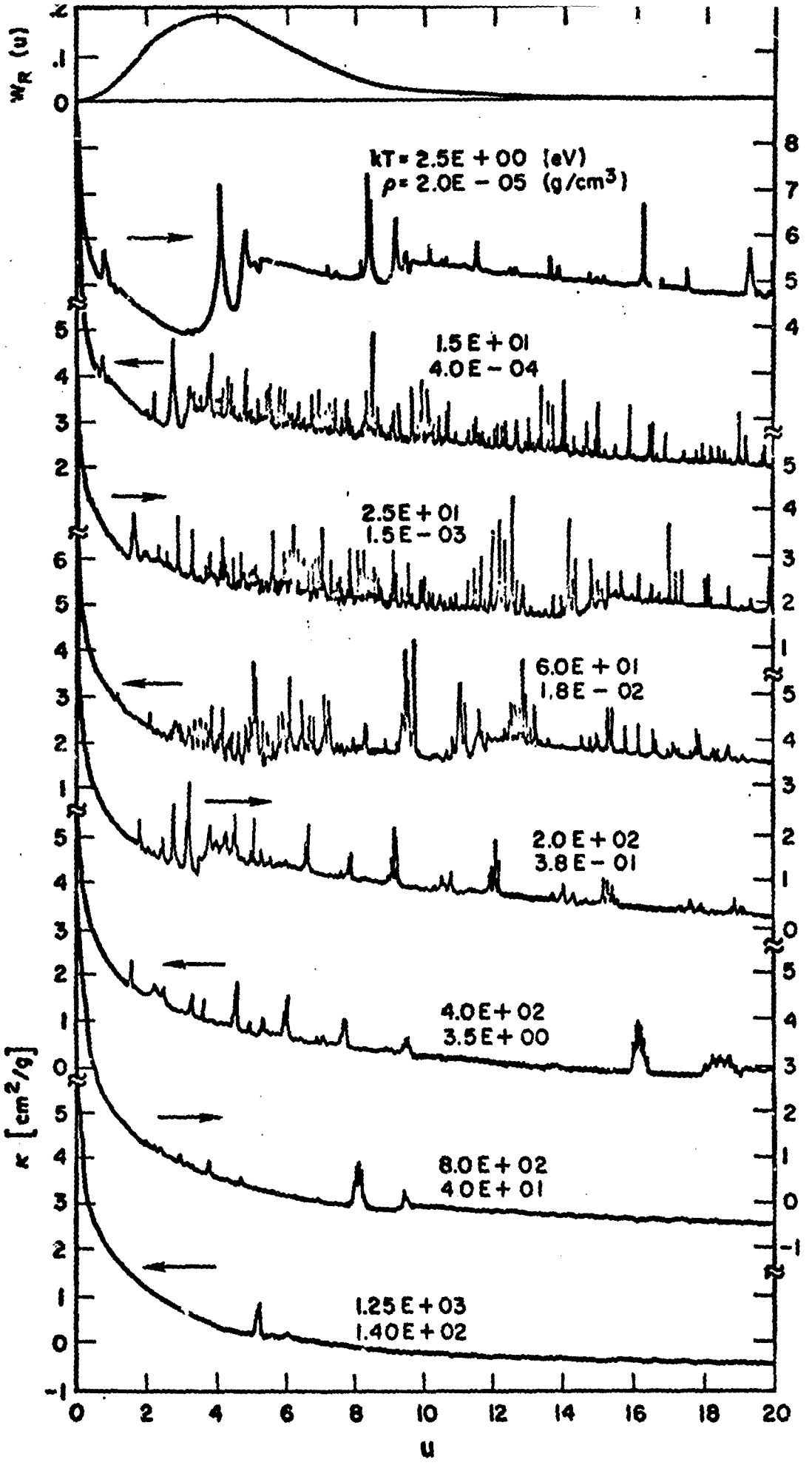
W_R (u)
kT = 2.5E + 00 (eV)
ρ = 2.0E − 05 (g/cm³)
1.5E + 01
4.0E − 04
2.5E + 01
1.5E − 03
6.0E + 01
1.8E − 02
2.0E + 02
3.8E − 01
4.0E + 02
3.5E + 00
8.0E + 02
4.0E + 01
1.25E + 03
1.40E + 02
κ [cm²/g]
u